USGS
science for a changing world

Prepared in cooperation with the Air Force Civil Engineer Center

Mapping the Altitude of the Top of the Dockum Group and Paleochannel Analysis Using Surface Geophysical Methods On and Near Cannon Air Force Base in Curry County, New Mexico, 2020

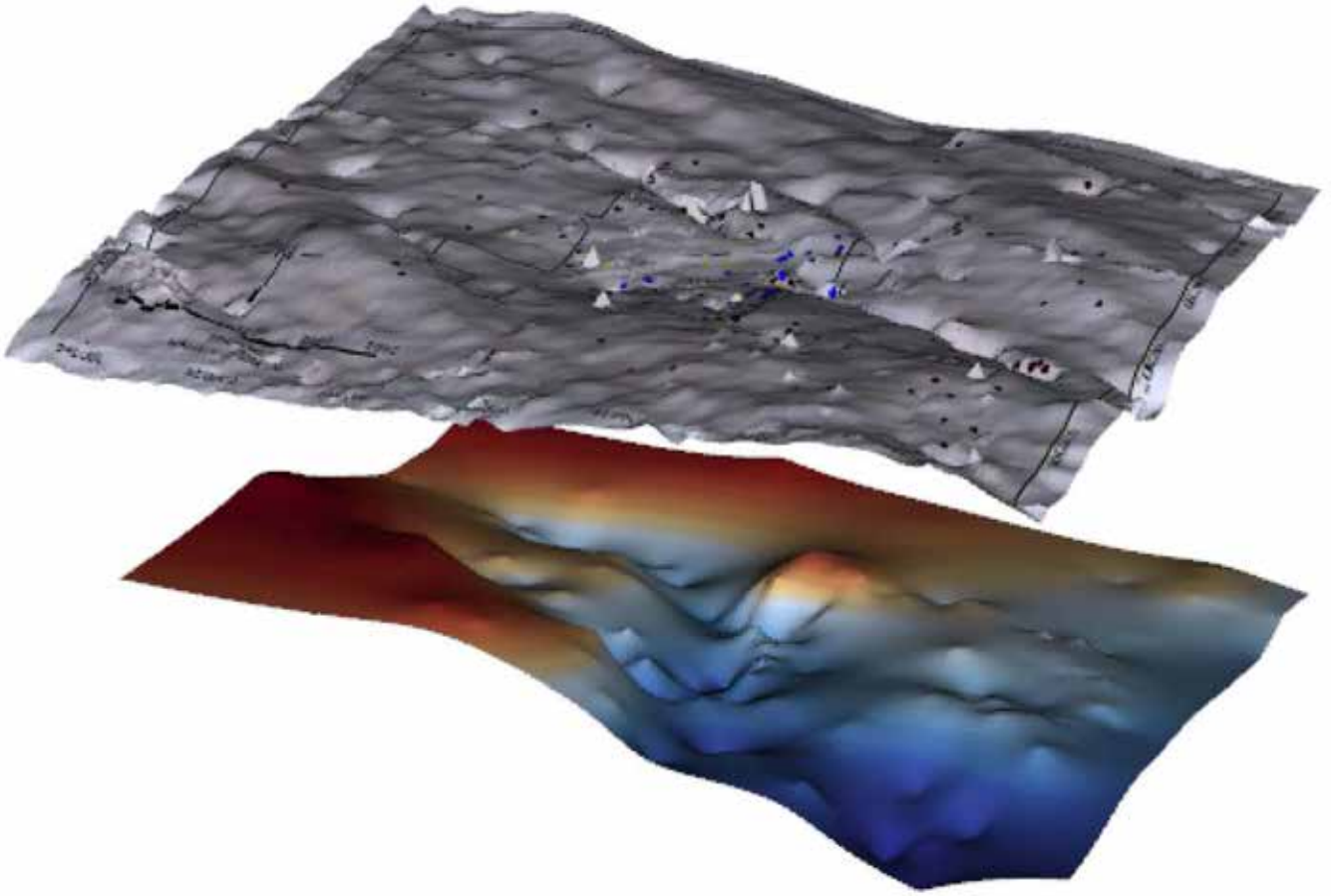

Scientific Investigations Report 2022–5050

U.S. Department of the Interior
U.S. Geological Survey

Cover. Three-dimensional model of the altitude of the top surface of Dockum Group (Chinle Formation) in relation to the land-surface altitude.

Mapping the Altitude of the Top of the Dockum Group and Paleochannel Analysis Using Surface Geophysical Methods On and Near Cannon Air Force Base in Curry County, New Mexico, 2020

By Jason D. Payne, Andrew P. Teeple, Jeremy McDowell, David Wallace, and Walker A. Hancock

Prepared in cooperation with the Air Force Civil Engineer Center

Scientific Investigations Report 2022–5050

U.S. Department of the Interior
U.S. Geological Survey

U.S. Geological Survey, Reston, Virginia: 2022

Suggested citation:
Payne, J.D., Teeple, A.P., McDowell, J., Wallace, D., and Hancock, W.A., 2022, Mapping the altitude of the top of the Dockum Group and paleochannel analysis using surface geophysical methods on and near Cannon Air Force Base in Curry County, New Mexico, 2020: U.S. Geological Survey Scientific Investigations Report 2022–5050, 21 p., https://doi.org/10.3133/sir20225050.

Associated data for this publication:
New Mexico Water Rights Reporting System, 2021, New Mexico Water Rights Reporting System: New Mexico Office of the State Engineer online database, accessed January 15, 2021, at http://nmwrrs.ose.state.nm.us/nmwrrs/wellSurfaceDiversion.html.

Payne, J.D., and Teeple, A.P., 2020, Surface geophysical data used for mapping the top of the Dockum Group on Cannon Air Force Base in Curry County, New Mexico, 2020: U.S. Geological Survey data release, https://doi.org/10.5066/P9P6KWR5.

U.S. Geological Survey, 2017, 1 meter digital elevation models (DEMs)—USGS National Map 3DEP downloadable data collection: U.S. Geological Survey data release, https://www.sciencebase.gov/catalog/item/543e6b86e4b0fd76af69cf4c.

ISSN 2328-0328 (online)

Contents

Figures

Tables

Conversion Factors

U.S. customary units to International System of Units

Multiply	By	To obtain
	Length	
inch (in.)	2.54	centimeter (cm)
inch (in.)	25.4	millimeter (mm)
foot (ft)	0.3048	meter (m)
mile (mi)	1.609	kilometer (km)
	Area	
acre	4,047	square meter (m^2)
acre	0.4047	hectare (ha)
acre	0.4047	square hectometer (hm^2)
acre	0.004047	square kilometer (km^2)

Temperature in degrees Celsius (°C) may be converted to degrees Fahrenheit (°F) as follows:

$$°F = (1.8 \times °C) + 32.$$

Temperature in degrees Fahrenheit (°F) may be converted to degrees Celsius (°C) as follows:

$$°C = (°F - 32) / 1.8.$$

Datum

Vertical coordinate information is referenced to the North American Vertical Datum of 1988 (NAVD 88).

Horizontal coordinate information is referenced to the North American Datum of 1983 (NAD 83) and to the World Geodetic System 1984 (WGS 84) datum.

Altitude, as used in this report, refers to distance above the vertical datum.

Abbreviations

AFB	Air Force Base
AECOM	Architecture, Engineering, Construction, Operations, and Management
EM	electromagnetic
Hz	hertz
NMWRRS	New Mexico Water Rights Reporting System
TDEM	time-domain electromagnetic
USGS	U.S. Geological Survey

Mapping the Altitude of the Top of the Dockum Group and Paleochannel Analysis Using Surface Geophysical Methods On and Near Cannon Air Force Base in Curry County, New Mexico, 2020

By Jason D. Payne, Andrew P. Teeple, Jeremy McDowell, David Wallace, and Walker A. Hancock

Abstract

The hydrogeology on and near Cannon Air Force Base (AFB) in eastern New Mexico was assessed to gain a better understanding of preferential groundwater flow paths through paleochannels. In and near the study area, paleochannels incised the top surface of the Dockum Group (Chinle Formation) and were subsequently filled in with electrically resistive coarse-grained sediments of the overlying Ogallala Formation, resulting in a preferential groundwater flow path in the form of a paleochannel network. A better understanding of the spatial characteristics of this preferential groundwater flow path is needed to support ongoing efforts to remediate groundwater contamination at Cannon AFB. Therefore, the U.S. Geological Survey, in cooperation with the U.S. Air Force Civil Engineer Center, used surface geophysical resistivity methods and data compiled from previous studies to better understand the spatial distribution and characteristics of the paleochannel network incised into the top of the Dockum Group.

Previous studies have shown these paleochannels incised into the top of the Dockum Group with increasing resolution, but limited borehole data on and near Cannon AFB continued to make accurately mapping the top of Dockum Group challenging. For this study, surface geophysical resistivity measurements in the form of time-domain electromagnetic soundings made by the U.S. Geological Survey were used in conjunction with data previously published by Architecture, Engineering, Construction, Operations, and Management and borehole data compiled from the New Mexico Water Rights Reporting System database to prepare an updated map of the top of the Dockum Group that includes the location and characteristics of paleochannels incised into the top of the Dockum Group (Chinle Formation). A total of 149 borehole picks (determinations of the tops and bases of geologic units and their hydrogeologic-unit equivalents) were obtained from previous studies, along with 72 additional borehole picks from the New Mexico Water Rights Reporting System database and 43 picks from newly collected time-domain electromagnetic soundings. The data were gridded and contoured using Oasis Montaj v. 9.8.1.

The updated map of the top of Dockum Group has many areas of uncertainty greater than 20 feet, because there are not enough data for the gridding process to reliably determine a value. However, this interpretation of the altitude of the top of the Dockum Group represents a substantial improvement in data resolution compared to previous studies.

Two methodologies were used to evaluate paleochannels incised in the top of the Dockum Group across the study area: (1) trend-removal grid analysis and (2) analysis with Esri's ArcMap Hydrology toolset. These two paleochannel analysis techniques show groundwater flow direction as well as areas having the deepest saturated thickness. Hydrologically, these techniques show where aquifer storage is highest (in the deepest parts of the paleochannel network), as well as the spatial distribution of preferential groundwater flow paths (the paleochannels). The analyses indicate a large paleochannel trending to the southeast, with smaller channels feeding in from the west. Areas where groundwater management could be more beneficial are indicated by locations where these flow lines intersect the deeper parts of the paleochannel.

Introduction

The hydrogeology on and near Cannon Air Force Base (AFB) in Curry County, New Mexico, was assessed to better understand preferential groundwater flow paths in the form of paleochannels. During the Triassic, streams cut channels into the geologic unit that formed the land surface at that time; remnants of these ancient streams remain in the form of paleochannels. On and near the study area, paleochannels incised the top surface of the Triassic-age Chinle Formation of Dockum Group and were subsequently filled with electrically resistive coarse-grained sediments from the overlying Tertiary-age Ogallala Formation (Rawlings, 2016), resulting in a

preferential groundwater flow path in the form of a paleochannel network. A better understanding of the spatial characteristics of this preferential groundwater flow path is needed to support ongoing efforts to remediate groundwater contamination at Cannon AFB. Chandra and others (2020, p. 1) explain "paleochannels typically act as pathways for groundwater movement and provide a potential source of groundwater. Their presence can be helpful in identifying areas suitable for recharge and at times in mitigating contamination problems in afflicted regions. Thus, mapping of paleochannels is significant in the planning and management of groundwater resources." Therefore, the U.S. Geological Survey (USGS), in cooperation with the U.S. Air Force Civil Engineer Center, used surface geophysical resistivity methods and data compiled from previous studies to better understand the spatial distribution and characteristics of the paleochannel network incised into the top of the Dockum Group.

Purpose and Scope

The primary purpose of this report is to update previously published depictions of the paleochannel network that traverses the top of Chinle Formation of the Dockum Group on and near Cannon AFB in Curry County, N. Mex. and functions as a preferential groundwater flow path. The altitude of the top of the Dockum Group was mapped, and spatial characteristics of the paleochannel network were described by using compiled and newly collected geophysical data.

Description of Study Area

The study area consists of about 35,000 acres on and near Cannon AFB in eastern New Mexico. Cannon AFB is approximately 7 miles southwest of Clovis, N. Mex., in the Southern High Plains physiographic province (Fenneman and Johnson, 1946; Langman and others, 2004). Cannon AFB is surrounded mostly by agricultural lands and dairy farms. The mean annual precipitation in Clovis during 1981–2020 was about 18 inches, and daily mean temperatures ranged from 78 degrees Fahrenheit in July to 39 degrees Fahrenheit in January (U.S. Climate Data, 2021). Mean annual evaporation rates in this semiarid region far exceed mean annual precipitation (Tuan and others, 1969; Robson and Banta, 1995). Cannon AFB covers approximately 3,800 acres and is host to the 27th Special Operations Group of the United States Air Force (Cannon Air Force Base, 2022) (fig. 1). Because of groundwater contamination related to historical operations at the site, an environmental restoration program is ongoing (Langman and others, 2004, 2006). Environmental restoration processes at Cannon AFB are being overseen by the Department of Defense (U.S. Government Accountability Office, 2021).

Geologic and Hydrogeologic Setting

The High Plains aquifer system is the largest aquifer in the United States and is commonly divided into three parts: the Northern High Plains aquifer, Central High Plains aquifer, and Southern High Plains aquifer (fig. 1) (Becker and others, 2002). The Southern High Plains aquifer underlies the study area. The High Plains aquifer system is commonly referred to as the "Ogallala aquifer" because the Ogallala Formation is the predominant water-bearing unit of this aquifer system (Gutentag and others, 1984).

Because the focus is on the hydrology of the area, geologic units are discussed from land surface downward (youngest to oldest), and aquifers and the geologic units that contain them are discussed together. The Quaternary-age Blackwater Draw Formation consists mostly of eolian sand deposits and overlies the Tertiary-age Ogallala Formation in the area; the Blackwater Draw Formation ranges in thickness from about 0 to 80 ft in eastern New Mexico (fig. 2; McLemore, 2001). The Blackwater Draw Formation is not considered a viable source of water in the study area. The Ogallala Formation consists of eolian sand and silt and fluvial and lacustrine sand, silt, clay, and gravel (McLemore, 2001), and ranges in thickness from about 30 to 600 ft in eastern New Mexico and western Texas (Gustavson, 1996). The Southern High Plains aquifer is the primary source of water for agriculture and public supply in the area and is primarily contained in the Ogallala Formation in eastern New Mexico (McLemore, 2001). The Ogallala Formation lies unconformably atop the upper unit of the eastward-dipping Triassic-age Chinle Formation of the Dockum Group (Dutton and Simpkins, 1986; Lucas and others, 1987). The Southern High Plains aquifer is underlain in most of the area by relatively impermeable rocks equivalent to the Chinle Formation (Cronin, 1969; Gutentag and others, 1984). The rocks that compose the Chinle Formation consist mostly of clay with some intermixed shale and silt that serve as barriers to groundwater movement (Cronin, 1969). The Chinle Formation ranges in thickness from about 0 to 400 feet (ft) in eastern New Mexico (McGowen and others, 1977). Locally, the Chinle Formation is referred to as the "red beds," an informal name commonly used for sedimentary rocks rich in ferric oxides (Neuendorf and others, 2005). The Triassic-age Santa Rosa Formation underlies the Chinle Formation. The Chinle Formation and the Santa Rosa Formation are the only members of the Dockum Group present in the study area. In addition to the Ogallala Formation, the Santa Rosa Formation is the other water-bearing member of the High Plains aquifer system present in the study area; the sandstone and shale aquifer is contained in the Santa Rosa Formation of the Dockum Group (Gustavson and Holliday, 1985) and is as a minor source of water, mostly for agricultural uses (New Mexico Interstate Stream Commission and New Mexico Office of the State Engineer, 2016). Although in New Mexico the water-bearing unit of the Dockum Group in the study area (the Santa Rosa Formation) is known as the sandstone and shale aquifer, the water-bearing unit of the Dockum Group

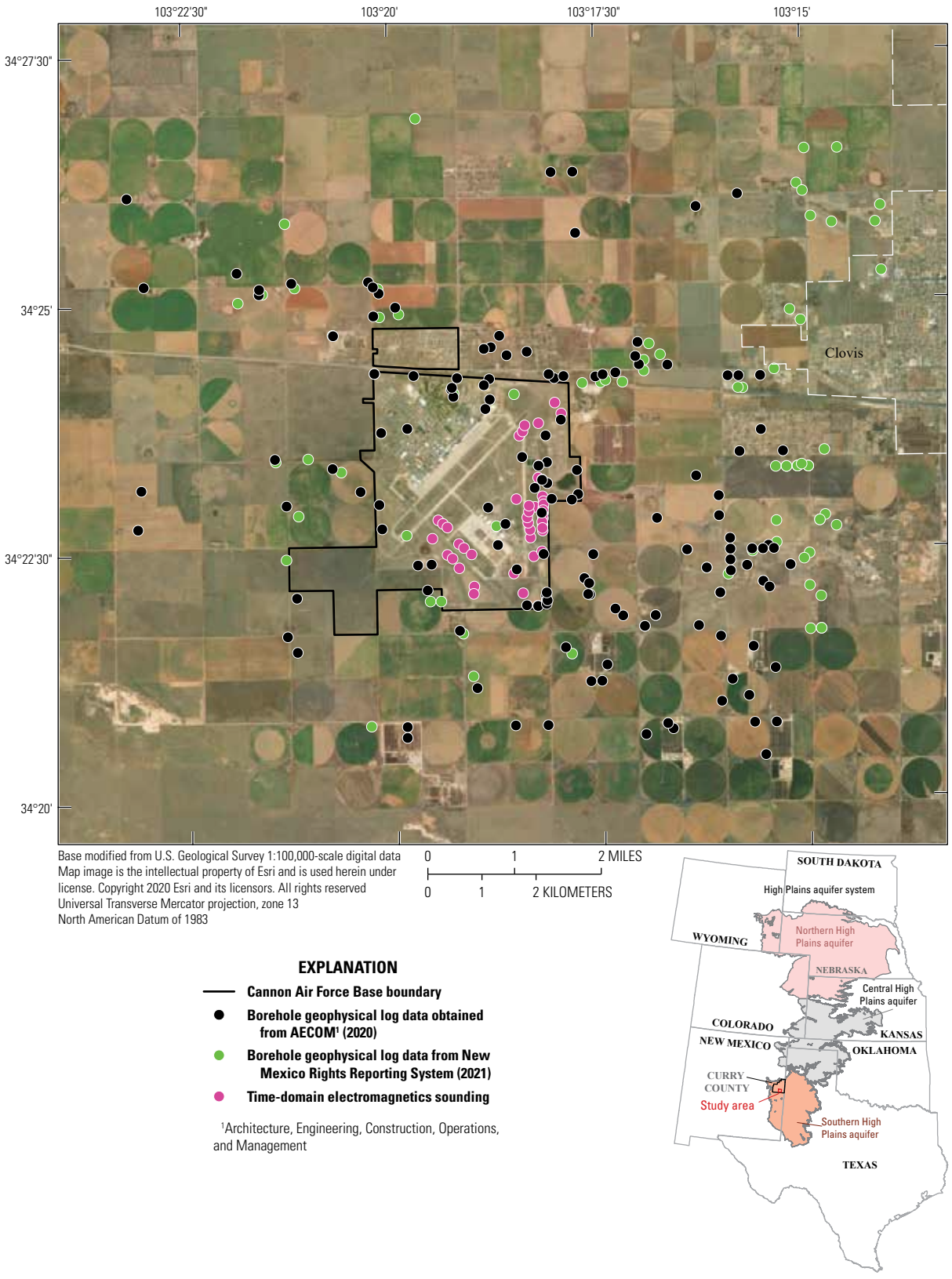

Figure 1. Locations of all boreholes and time-domain electromagnetic (TDEM) soundings on and near Cannon Air Force Base in Curry County, New Mexico, 2020.

is known as the Dockum aquifer in Texas (Matherne and Stewart, 2012; New Mexico Interstate Stream Commission and New Mexico Office of the State Engineer, 2016).

The hydrogeologic setting on and near Cannon AFB is the complex result of the Laramide orogeny between 80 and 55 million years ago that formed the Rocky Mountains and possibly earlier orogenies as well that predate the Laramide orogeny (Gustavson and Holliday, 1985). Prior to the Laramide orogeny, eastern New Mexico and the Texas Panhandle were covered by a large sea that was part of the Western Interior Seaway, which deposited the Dockum Group sediments during the Triassic period (Gustavson and Holliday, 1985). The Dockum Group is composed of sandstone with interbedded shales grading upward to a shaly sandstone or siltstone and clay (Luckey and Becker, 1999). When the Laramide orogeny began and the Western Interior Seaway regressed, the area on and near the present-day Cannon AFB was traversed by large rivers that had their headwaters in the Rocky Mountains and predominately flowed in an east-southeast direction. These rivers downcut into the Chinle Formation that forms the upper part of the Dockum Group until the late Miocene epoch (Gustavson and Holliday, 1985) when the incised channels began to fill with fluvial sediments such as sand and gravel originating from the Rocky Mountain headwaters; subsequent to channel incision and streambed sediment deposition, sand and gravel deposits from complex ancestral alluvial fan systems were deposited and then reworked to form the overlying Ogallala Formation (Knowles and others, 1984).

Previous Studies

The USGS has conducted several assessments in recent years to characterize the hydrogeology on and near Cannon AFB. Data and information from previous studies were used to guide the assessment described herein. Previous USGS studies include Collison (2016), Langman and others (2006), and Langman and others (2004). A previous study by Architecture, Engineering, Construction, Operations, and Management (AECOM, 2020) assessed the location of the paleochannels on and near Cannon AFB by using available borehole data from the New Mexico Water Rights Reporting System (NMWRRS) database and the Cannon AFB Installation Restoration Program. In 2018, the USGS collected geophysical logs from 21 existing boreholes and from 4 new boreholes at the Cannon AFB as well as 4 new test wells (available through the USGS GeoLog Locator system at https://doi.org/10.5066/F7X63KT0). Those data were incorporated in this report and were also used in AECOM (2020), which describes the spatial distribution paleochannels at Cannon AFB by using available borehole data. AECOM (2020) discusses limitations of their final map resulting from gaps in the borehole data that they used in their analysis. The data used to develop their interpretation of the spatial distribution of paleochannels in the top of the Dockum Group are among the data incorporated in the development of the updated interpretation of the spatial distribution of paleochannels in top of Dockum Group described in this report.

Era	Period	Geologic unit		Lithologic description	Hydrogeologic unit
Cenozoic	Quaternary	Blackwater Draw Formation[2]		Eolian sand deposits[3]	([1])
	Tertiary	Ogallala Formation		Eolian sand and silt and fluvial and lacustrine sand, silt, clay, and gravel[3]	Southern High Plains aquifer
Mesozoic	Triassic	Dockum Group	Chinle Formation	Clay with some intermixed sand and silt[4]	([5])
			Santa Rosa Formation	Sandstone with interbedded shales grading upward to a shaly sandstone or siltstone[6]	Sandstone and shale aquifer[7 8]

[1]Not applicable.
[2]The unconfined Southern High Plains aquifer in New Mexico is composed primarily of the Ogallala Formation (McLemore, 2001).
[3]McLemore (2001).
[4]Dutton and Simpkins (1986).
[5]Barrier to groundwater movement between the Southern High Plains aquifer and the sandstone and shale aquifer.
[6]Luckey and Becker (1999).
[7]Matherne and Stewart (2012).
[8]New Mexico Interstate Stream Commission and New Mexico Office of the State Engineer (2016).

Figure 2. Geology of the near-surface (top) geologic units and their hydrogeologic-unit equivalents on and near Cannon Air Force Base, Curry County, New Mexico (modified from Matherne and Stewart, 2012).

Data Collection, Compilation, and Processing Methods

Resistivity measurements are commonly used to interpolate geologic and hydrogeologic properties between borehole locations or in areas where no borehole data exist. Data from surface geophysical resistivity methods were used to fill data gaps pertaining to the spatial distribution of paleochannels at Cannon AFB. Surface geophysical resistivity measurements in the form of time-domain electromagnetic (TDEM) soundings made by the USGS were published as a companion data release to this report (Payne and Teeple, 2020). These TDEM soundings were used in conjunction with data published in AECOM (2020) and borehole data compiled from NMWRRS (2021) to prepare an updated map of the top of the Dockum Group that includes the location and characteristics of paleochannels incised into the top of the Dockum Group (Chinle Formation).

TDEM Soundings

TDEM instruments measure the bulk resistivity of the subsurface by producing an alternating electrical current in a transmitter loop of wire deployed on the land surface (Vignesh and others, 2015). TDEM soundings in this study were collected using the Geonics Protem 47 and 57 systems, respectively (Geonics Limited, 2006). Both systems use a multiturn receiver coil to measure electromagnetic (EM) fields in the center of the transmitter loop. The TDEM soundings were collected at two frequencies using the Geonics Protem 47 (285 and 75 hertz [Hz]) and three frequencies using the Geonics Protem 57 (30, 7.5, and 3.0 Hz) for a total of five frequencies. The lower frequencies penetrate deeper into the subsurface. For each frequency, 10 stacks (independent measurements) were collected by using an integration time of either 8 or 15 seconds, the latter of which was used for collecting 3.0-Hz data with the Geonics Protem 57. Longer integration time helps improve signal to noise ratio, thereby compensating for the dissipation of the transmitted signal at depth and for the greater potential for EM background noise with these soundings compared to soundings collected at higher frequencies (shallower depths). Additional information about the TDEM method and data collected in this study are available in Payne and Teeple (2020). The TDEM data were collected in accordance with methods defined by the American Society of Testing and Materials (1999). Comprehensive descriptions of the theory and application of geophysical resistivity methods, as well as tables of the electrical properties of earth materials, are presented in Keller and Frischknecht (1966) and Lucius and others (2007) and will not be detailed in this report.

Sixty TDEM soundings, 43 of which were used in the final interpretation, were collected at Cannon AFB (fig. 1) to supplement existing borehole data. TDEM transmitter loops covering 100 square meters were used to ensure that the depth of exploration would accurately image the electrically conductive Chinle Formation. For each TDEM sounding, the voltages measured from the eddy currents were averaged and evaluated statistically by using preprocessing scripts that incorporate raw field data (namely, voltage data) and independently compute the uncertainty of each time gate. A time gate is defined as one of multiple time windows (after current shutoff) during which discrete voltages are measured. Variability observed in a time gate can represent signal noise or a systematic change not representative of stable data (Mandache and Brothers, 2005).

In this application, 10 percent of the data from each tail of the distribution were removed, and an average of the remaining 80 percent was computed. The resulting averages were then compared to a noise sample collected at the sounding location, and any values that were less than half of the associated EM background noise value were removed from the final sounding. The final averaged values for each time gate were saved as processed data files and used for inverse modeling whereby the spatial distribution of subsurface resistivity was estimated from the measured voltage. The IX1D v3 program, developed by Interpex Limited (1996), was used for inverse modeling of the TDEM soundings. A smooth inverse model—defined as a multilayered model that holds the depth values fixed and allows the resistivity values to vary during inversion—was fit to the data by using Occam's inversion principle (Constable and others, 1987). Layered-earth models, which are simplified models used to represent hydrogeologic units, were then generated and fit to the data to better represent the electrical stratigraphy of each sounding. The changes in resistivity from the inverse modeling results of the final processed TDEM data were used to determine changes in hydrogeologic contacts, namely the tops and bases of hydrogeologic units. More detailed descriptions of the field procedures, equipment setup, and processing steps used to develop one-dimensional soundings (commonly referred to as "virtual borehole resistivity logs") from the TDEM soundings are available in the data release that accompanies this report (Payne and Teeple, 2020).

Each of the 60 soundings was evaluated for accuracy by first looking at the background EM noise in the location of the sounding. This evaluation led to the removal of eight soundings from the dataset because the noise level overwhelmed any measurable signal. The remaining soundings were then carefully analyzed and compared to nearby borehole data. This additional scrutiny and comparison to nearby borehole data led to the removal of nine additional soundings from the dataset. For all removed soundings, the depth to top of the Dockum Group differed from the depth in nearby boreholes by more than 10 ft; this large difference in depth helped to confirm the decision to remove these soundings from the dataset was the correct decision. All TDEM sounding locations are listed in table 1; the TDEM soundings that were used in the analysis include depth and altitude values for the top of the Dockum Group.

Table 1. Location, depth to top of Dockum Group, and altitude of the top of Dockum Group for the time-domain electromagnetic (TDEM) soundings used in the final interpretation (Payne and Teeple, 2020).

[ID, identifier; WGS 84, World Geodetic System 1984; --, data not available because sounding was not used in final interpretation]

Site ID	Longitude, WGS 84 datum (decimal degrees)	Latitude, WGS 84 datum (decimal degrees)	Land surface altitude (feet)	Depth to top of Dockum Group (feet)	Top of Dockum Group altitude (feet)
TDEM01	−103.30483	34.38232	4,276	403	3,873
TDEM02	−103.30527	34.37405	4,268	398	3,870
TDEM03	−103.30437	34.38837	4,274	--	--
TDEM04	−103.30412	34.38720	4,285	359	3,926
TDEM05	−103.30393	34.38623	4,285	--	--
TDEM06	−103.30355	34.38498	4,275	--	--
TDEM07	−103.30330	34.38407	4,275	336	3,939
TDEM08	−103.30312	34.38323	4,275	356	3,919
TDEM09	−103.30317	34.38223	4,274	357	3,917
TDEM10	−103.30323	34.38130	4,274	346	3,928
TDEM11	−103.30328	34.38037	4,274	360	3,914
TDEM12	−103.30338	34.37935	4,273	365	3,908
TDEM13	−103.30337	34.37832	4,272	355	3,917
TDEM14	−103.30752	34.36790	4,264	392	3,872
TDEM15	−103.30932	34.37123	4,265	389	3,876
TDEM16	−103.30658	34.36967	4,266	--	--
TDEM17	−103.30535	34.36790	4,266	--	--
TDEM18	−103.33008	34.38073	4,279	--	--
TDEM19	−103.32565	34.37727	4,268	361	3,907
TDEM20	−103.32267	34.37452	4,268	365	3,903
TDEM21	−103.32165	34.37387	4,269	362	3,907
TDEM22	−103.32033	34.37225	4,270	373	3,897
TDEM23	−103.31735	34.36915	4,267	403	3,864
TDEM24	−103.31477	34.36758	4,266	--	--
TDEM25	−103.32442	34.38033	4,277	348	3,929
TDEM26	−103.32348	34.37972	4,275	339	3,936
TDEM27	−103.32260	34.37910	4,274	348	3,926
TDEM28	−103.32032	34.37632	4,270	337	3,933
TDEM29	−103.31932	34.37563	4,271	338	3,933
TDEM30	−103.31780	34.37453	4,270	351	3,919
TDEM31	−103.31748	34.36793	4,268	396	3,872
TDEM32	−103.29897	34.40162	4,310	--	--
TDEM33	−103.30053	34.39972	4,311	372	3,939
TDEM34	−103.29925	34.39788	4,305	362	3,943
TDEM35	−103.29735	34.38978	4,279	--	--
TDEM36	−103.29650	34.38875	4,273	--	--
TDEM37	−103.29645	34.38537	4,266	--	--
TDEM38	−103.30858	34.38367	4,275	394	3,881
TDEM39	−103.30357	34.37487	4,270	371	3,899
TDEM40	−103.31690	34.38690	4,285	--	--
TDEM41	−103.31383	34.38858	4,284	--	--

Table 1. Location, depth to top of Dockum Group, and altitude of the top of Dockum Group for the time-domain electromagnetic (TDEM) soundings used in the final interpretation (Payne and Teeple, 2020).—Continued

[ID, identifier; WGS 84, World Geodetic System 1984; --, data not available because sounding was not used in final interpretation]

Site ID	Longitude, WGS 84 datum (decimal degrees)	Latitude, WGS 84 datum (decimal degrees)	Land surface altitude (feet)	Depth to top of Dockum Group (feet)	Top of Dockum Group altitude (feet)
TDEM42	−103.31217	34.38967	4,286	--	--
TDEM43	−103.30780	34.39427	4,288	411	3,877
TDEM44	−103.30710	34.39497	4,291	427	3,864
TDEM45	−103.30667	34.39598	4,293	407	3,886
TDEM46	−103.30390	34.39632	4,297	385	3,912
TDEM47	−103.30312	34.38272	4,274	359	3,915
TDEM48	−103.30323	34.38175	4,274	354	3,920
TDEM49	−103.30333	34.38080	4,274	369	3,905
TDEM50	−103.30345	34.37983	4,274	373	3,901
TDEM51	−103.30342	34.37877	4,272	363	3,909
TDEM52	−103.31287	34.38687	4,281	--	--
TDEM53	−103.30510	34.37145	4,271	--	--
TDEM54	−103.30585	34.37720	4,269	422	3,847
TDEM55	−103.30593	34.37850	4,270	431	3,839
TDEM56	−103.30628	34.37968	4,274	439	3,835
TDEM57	−103.30645	34.38057	4,273	426	3,847
TDEM58	−103.30610	34.38157	4,272	420	3,852
TDEM59	−103.30607	34.38252	4,273	412	3,861
TDEM60	−103.30585	34.38595	4,285	--	--

Data Compilation

Table 2 lists the altitude of the top of the Dockum Group as interpreted from all boreholes in the study area. (All of the data in table 2 are from AECOM, 2020.) AECOM (2020) computed the top of Dockum Group altitude (shown in table 2) by subtracting the depth to the top of the Chinle Formation from a 1-meter (m) digital elevation model (U.S. Geological Survey, 2017). Because of the possible discrepancies between surface altitudes used by AECOM and those used in this report, actual altitudes of the top of the Dockum Group may differ slightly.

To supplement the AECOM (2020) dataset, a search of the NMWRRS database revealed an additional 72 wells near Cannon AFB that included drillers' descriptions of the depth at which the top of the Dockum Group was reached (NMWRRS, 2021). As with the AECOM data, these depths were subtracted from the regional 1-m digital elevation model to produce additional control points in the final depiction of the top of Dockum Group. The borehole data obtained from the NMWRRS database that were used in the final interpretation in this report are provided in table 3.

Table 2. Location, depth to top of Dockum Group, and altitude of the top of Dockum Group from Architecture, Engineering, Construction, Operations, and Management (AECOM, 2020).

[ID, identifier; WGS 84, World Geodetic System 1984]

Site ID	Longitude, WGS 84 datum (decimal degrees)	Latitude, WGS 84 datum (decimal degrees)	Land surface altitude (feet)	Depth to top of Dockum Group (feet)	Top of Dockum Group altitude (feet)
CC1050	−103.26334	34.40376	4,319	400	3,919
CC1542	−103.25902	34.36931	4,238	350	3,888
CC364S	−103.27215	34.36207	4,258	375	3,883
CC403POD8	−103.29185	34.35303	4,258	400	3,858
MW-A	−103.30873	34.37191	4,267	339	3,928
MW-M	−103.30280	34.36665	4,264	287	3,978
MW-F	−103.30398	34.38925	4,278	368	3,910
CC2191POD1	−103.31466	34.40888	4,330	354	3,976
CC1264	−103.25898	34.37474	4,244	302	3,942
MW-D	−103.30679	34.36587	4,265	355	3,910
MW-H	−103.30484	34.38548	4,279	348	3,931
MW-Fa	−103.30453	34.36572	4,266	350	3,916
CC01574	−103.31150	34.41104	4,324	405	3,919
CC873	−103.31008	34.40777	4,327	335	3,992
CC142S	−103.26117	34.34574	4,227	346	3,881
CC02191POD1	−103.31324	34.40915	4,330	354	3,976
BH-3	−103.30351	34.38133	4,274	378	3,896
PW-12	−103.31363	34.40040	4,311	404	3,907
PW-8	−103.32017	34.40406	4,321	415	3,906
PW-6	−103.32590	34.37293	4,269	360	3,909
CC293POD7	−103.26775	34.34935	4,242	430	3,812
CC164	−103.29908	34.35874	4,264	407	3,857
CC1315	−103.30286	34.34575	4,242	362	3,880
CC1868	−103.26774	34.36024	4,259	402	3,857
MW-Pa	−103.30229	34.38625	4,274	360	3,914
PW-5	−103.30247	34.39425	4,294	385	3,909
CC1320S	−103.25681	34.35483	4,246	410	3,836
CC142S2	−103.25903	34.34029	4,211	397	3,814
CC00451S6	−103.35992	34.41849	4,366	432	3,934
CC303S2	−103.28312	34.34398	4,241	360	3,881
MW-Ga	−103.30401	34.38920	4,279	360	3,919
BH-4	−103.30327	34.37441	4,270	393	3,877
CC1857	−103.29223	34.40399	4,306	348	3,958
OW-1	−103.32138	34.40217	4,318	414	3,904
CC1610	−103.26551	34.40379	4,318	378	3,940
CC1761	−103.26773	34.36750	4,255	341	3,914
CC02095POD1	−103.26773	34.38041	4,243	330	3,913
CC1499	−103.26554	34.37478	4,245	322	3,923
CC114S3	−103.36433	34.42214	4,376	437	3,939
CC122S	−103.33242	34.41603	4,347	438	3,909
PW-4a	−103.32123	34.40246	4,321	416	3,905

Table 2. Location, depth to top of Dockum Group, and altitude of the top of Dockum Group from Architecture, Engineering, Construction, Operations, and Management (AECOM, 2020).—Continued

[ID, identifier; WGS 84, World Geodetic System 1984]

Site ID	Longitude, WGS 84 datum (decimal degrees)	Latitude, WGS 84 datum (decimal degrees)	Land surface altitude (feet)	Depth to top of Dockum Group (feet)	Top of Dockum Group altitude (feet)
CC01476POD4	−103.28306	34.36210	4,260	370	3,890
CC1476POD4	−103.28306	34.36210	4,260	370	3,890
CC317S	−103.35332	34.42031	4,369	452	3,917
CC563	−103.28360	34.40963	4,330	388	3,942
CC2056POD6	−103.34506	34.41143	4,324	382	3,942
CC1182	−103.26223	34.37203	4,241	320	3,921
GTW-2	−103.29610	34.38433	4,270	365	3,905
CC1901	−103.35499	34.38305	4,297	348	3,949
CC1190	−103.34557	34.38919	4,309	365	3,944
CC1069	−103.28340	34.40590	4,322	373	3,949
CC122POD8	−103.33687	34.41462	4,345	423	3,922
CC1995	−103.29075	34.40431	4,308	350	3,958
CC1105POD7	−103.33130	34.34400	4,230	248	3,982
CC2235POD1	−103.33575	34.37897	4,279	335	3,944
MW-G	−103.30332	34.38687	4,279	358	3,921
CC142S3	−103.28896	34.36507	4,260	370	3,890
CC971	−103.35719	34.39089	4,320	360	3,960
CC1326	−103.26115	34.37477	4,246	321	3,925
PW-3	−103.31455	34.39882	4,306	400	3,906
CC02386	−103.33780	34.42036	4,357	435	3,922
BH-2	−103.31086	34.37953	4,273	391	3,882
CC119S4	−103.26300	34.43422	4,353	406	3,947
CC366S6	−103.25677	34.34574	4,222	394	3,828
MW-Sa	−103.30280	34.36606	4,263	362	3,901
CC1538	−103.26338	34.39109	4,283	345	3,938
GTW-3	−103.31476	34.40281	4,318	389	3,929
CC142S4	−103.29441	34.36759	4,261	363	3,898
CC02093POD1	−103.28025	34.38013	4,252	328	3,924
MW-Na	−103.29628	34.38836	4,269	355	3,914
CC00145S4	−103.29403	34.36751	4,261	363	3,898
PW-4	−103.32097	34.40095	4,311	400	3,911
CC1032POD7	−103.34000	34.38527	4,299	349	3,950
CC00145S3	−103.28742	34.36391	4,260	370	3,890
PW-2	−103.32893	34.40455	4,307	375	3,932
CC875	−103.30166	34.40449	4,316	342	3,974
MW-W	−103.29739	34.38343	4,273	364	3,909
CC1551	−103.29583	34.42805	4,362	395	3,967
CC02094POD1	−103.26772	34.38374	4,261	333	3,928
CC933	−103.35320	34.35853	4,279	273	4,006
CC303POD3	−103.27762	34.34487	4,244	375	3,869
GTW-1	−103.33567	34.39508	4,319	355	3,964

Table 2. Location, depth to top of Dockum Group, and altitude of the top of Dockum Group from Architecture, Engineering, Construction, Operations, and Management (AECOM, 2020).—Continued

[ID, identifier; WGS 84, World Geodetic System 1984]

Site ID	Longitude, WGS 84 datum (decimal degrees)	Latitude, WGS 84 datum (decimal degrees)	Land surface altitude (feet)	Depth to top of Dockum Group (feet)	Top of Dockum Group altitude (feet)
CC1990POD1	−103.38314	34.41997	4,382	410	3,972
CC865	−103.27765	34.40575	4,324	370	3,954
BH-1	−103.31431	34.38233	4,274	376	3,898
CC403A	−103.29075	34.35575	4,260	377	3,883
CC856	−103.26557	34.37298	4,249	322	3,927
CC1339	−103.29325	34.37424	4,270	360	3,910
CC2472	−103.27141	34.43222	4,352	395	3,957
CC01864	−103.27429	34.37478	4,256	327	3,929
CC1864	−103.27429	34.37478	4,256	327	3,929
CC1516	−103.30057	34.43830	4,365	387	3,978
CC1411	−103.29619	34.43830	4,378	401	3,977
CC1072	−103.28412	34.40728	4,328	378	3,950
CC802	−103.25676	34.37477	4,246	323	3,923
CC1855	−103.25899	34.39470	4,302	360	3,942
MW-Y	−103.30145	34.38361	4,273	357	3,916
CC1180S	−103.35514	34.36116	4,287	276	4,011
CC142S5	−103.29416	34.36941	4,264	358	3,906
CC00875	−103.30055	34.40381	4,313	340	3,973
MW-Ta	−103.30262	34.36664	4,264	361	3,903
CC792	−103.25779	34.36833	4,242	317	3,925
CC914	−103.26553	34.37115	4,250	323	3,927
CC743	−103.31705	34.35213	4,250	291	3,959
PW-9	−103.31244	34.37603	4,273	378	3,895
CC1026	−103.35318	34.36759	4,281	270	4,011
EB-1	−103.33625	34.38305	4,290	335	3,955
CC757	−103.28817	34.40460	4,314	355	3,959
CC114S8	−103.38632	34.43487	4,413	422	3,991
CC293	−103.26554	34.35300	4,251	408	3,843
CC02014POD1	−103.27038	34.37169	4,254	323	3,931
CC2014POD1	−103.27038	34.37169	4,254	323	3,931
CC2120POD1	−103.38425	34.38592	4,322	292	4,030
PW-7	−103.33037	34.39571	4,322	368	3,954
CC293S5	−103.26224	34.35025	4,241	403	3,838
CC293A	−103.26119	34.35846	4,259	390	3,869
MW-V	−103.33684	34.40500	4,328	370	3,958
CC00145S5	−103.29512	34.37025	4,266	358	3,908
CC112S3	−103.35984	34.41934	4,366	426	3,940
CC688	−103.32041	34.36178	4,265	302	3,963
CC1046	−103.25902	34.36931	4,238	309	3,929
CC1070	−103.29406	34.35300	4,259	371	3,888
MW-C	−103.30458	34.36574	4,267	360	3,907

Table 2. Location, depth to top of Dockum Group, and altitude of the top of Dockum Group from Architecture, Engineering, Construction, Operations, and Management (AECOM, 2020).—Continued

[ID, identifier; WGS 84, World Geodetic System 1984]

Site ID	Longitude, WGS 84 datum (decimal degrees)	Latitude, WGS 84 datum (decimal degrees)	Land surface altitude (feet)	Depth to top of Dockum Group (feet)	Top of Dockum Group altitude (feet)
CC01476S	−103.28085	34.36387	4,262	355	3,907
CC1476S	−103.28085	34.36387	4,262	355	3,907
CC00873	−103.30600	34.40831	4,321	335	3,986
CC241S4	−103.38503	34.37942	4,322	285	4,037
CC318S5	−103.30942	34.34579	4,237	305	3,932
CC1558	−103.25461	34.39107	4,289	350	3,939
MW-V	−103.33684	34.40500	4,328	369	3,959
CC00623	−103.31368	34.40382	4,321	374	3,947
CC00015POD5	−103.27222	34.38714	4,268	318	3,950
CC951	−103.25346	34.37201	4,250	324	3,926
CC1105POD5	−103.33126	34.34580	4,236	247	3,989
MW-Oa	−103.29934	34.39684	4,300	364	3,936
MW-B	−103.30288	34.36741	4,265	360	3,905
MW-Ca	−103.30228	34.38975	4,275	350	3,925
MW-Ua	−103.30275	34.36796	4,265	361	3,904
MW-X	−103.32865	34.37282	4,268	335	3,933
CC280S	−103.26557	34.37660	4,248	320	3,928
CC2160POD2	−103.29867	34.40413	4,308	330	3,978
CC650S	−103.32678	34.36863	4,267	322	3,945
CC122S6	−103.33687	34.41949	4,356	428	3,928
MW-E	−103.30729	34.39070	4,283	346	3,937
CC00122POD7	−103.33571	34.41843	4,355	428	3,927
MW-Rb	−103.30331	34.38681	4,279	350	3,929
CC1266	−103.26773	34.36750	4,255	329	3,926
CC1142	−103.25896	34.40376	4,320	375	3,945
CC303S3	−103.27870	34.34578	4,245	360	3,885

Table 3. Location, depth to top of Dockum Group, and altitude of the top of Dockum Group obtained from the New Mexico Water Rights Reporting System (NMWRRS, 2021).

[ID, identifier; WGS 84, World Geodetic System 1984]

Site ID	Longitude, WGS 84 datum (decimal degrees)	Latitude, WGS 84 datum (decimal degrees)	Land surface altitude (feet)	Depth to top of Dockum Group (feet)	Top of Dockum Group altitude (feet)
CC01156	−103.32470	34.36752	4,267	295	3,972
L14689POD1	−103.33147	34.37863	4,278	193	4,085
CC00909POD2	−103.31334	34.38000	4,274	395	3,879
CC00164	−103.29847	34.35845	4,264	407	3,857
CC02222POD1	−103.26319	34.40253	4,316	380	3,936
CC02574POD1	−103.33652	34.41999	4,357	440	3,917
CC00122POD2	−103.33240	34.41567	4,346	438	3,908
CC00601	−103.24467	34.37927	4,232	323	3,909
CC00563	−103.28195	34.41016	4,331	388	3,943
CC01901	−103.35321	34.38212	4,294	348	3,946
CC02231POD1	−103.32153	34.40230	4,319	414	3,905
CC01743	−103.25457	34.38925	4,278	347	3,931
CC01002	−103.25130	34.37385	4,243	328	3,915
CC00317S	−103.35332	34.42031	4,369	452	3,917
CC01875POD2	−103.24804	34.36207	4,236	328	3,908
CC00630	−103.23479	34.42191	4,315	403	3,912
CC01995	−103.29083	34.40416	4,308	350	3,958
CC01857	−103.29180	34.40380	4,307	348	3,959
CC01738	−103.25674	34.38928	4,277	345	3,932
CC01782	−103.25017	34.38925	4,280	350	3,930
CC01069	−103.28307	34.40563	4,322	373	3,949
CC02502POD1	−103.25150	34.38960	4,282	350	3,932
CC00650S	−103.32687	34.36755	4,266	322	3,944
CC00280POD7	−103.25680	34.37659	4,249	330	3,919
CC01746	−103.24799	34.36749	4,241	330	3,911
CC01041	−103.25676	34.40561	4,326	400	3,926
CC01190	−103.34445	34.38938	4,310	365	3,945
CC00021POD3	−103.24333	34.44249	4,343	390	3,953
CC00558	−103.24464	34.43005	4,322	380	3,942
CC00280POD8	−103.25679	34.38023	4,253	336	3,917
CC00629	−103.25125	34.41376	4,325	398	3,927
CC00971	−103.35766	34.39123	4,321	360	3,961
CC00649	−103.24688	34.39199	4,280	353	3,927
CC00636	−103.23587	34.43004	4,324	390	3,934
CC00786	−103.24801	34.38022	4,250	326	3,924
CC02577POD1	−103.31842	34.35491	4,254	295	3,959
CC01105POD18	−103.33914	34.34677	4,239	242	3,997
CC00745	−103.25342	34.41554	4,327	394	3,933
CC01980POD1	−103.26667	34.37139	4,252	324	3,928
CC00757	−103.28741	34.40380	4,312	355	3,957
CC00814S	−103.25167	34.43666	4,341	380	3,961

Table 3. Location, depth to top of Dockum Group, and altitude of the top of Dockum Group obtained from the New Mexico Water Rights Reporting System (NMWRRS, 2021).—Continued

[ID, identifier; WGS 84, World Geodetic System 1984]

Site ID	Longitude, WGS 84 datum (decimal degrees)	Latitude, WGS 84 datum (decimal degrees)	Land surface altitude (feet)	Depth to top of Dockum Group (feet)	Top of Dockum Group altitude (feet)
CC01772	−103.25235	34.38928	4,279	345	3,934
CC01780	−103.25235	34.38928	4,279	345	3,934
CC01783	−103.25235	34.38928	4,279	345	3,934
CC01431	−103.25024	34.36930	4,244	327	3,917
CC01452	−103.23479	34.43279	4,328	386	3,942
CC01072	−103.28303	34.40743	4,328	378	3,950
CC02142POD1	−103.25050	34.43538	4,336	376	3,960
CC00069POD2	−103.24889	34.43110	4,329	374	3,955
CC00021POD2	−103.25000	34.44250	4,349	384	3,965
CC01217	−103.24801	34.38022	4,250	324	3,926
CC00122POD8	−103.33630	34.41525	4,347	423	3,924
CC00981	−103.25020	34.37473	4,240	320	3,920
CC00112S3	−103.35984	34.41934	4,366	426	3,940
CC00112POD8	−103.36481	34.41794	4,358	402	3,956
CC01032POD6	−103.35112	34.39166	4,320	354	3,966
CC01781	−103.25017	34.38925	4,280	345	3,935
CC00950	−103.24690	34.38111	4,251	324	3,927
CC01461	−103.24804	34.36207	4,236	322	3,914
CC02530POD1	−103.26170	34.37519	4,250	320	3,930
CC00688	−103.32036	34.36209	4,265	302	3,963
CC01763	−103.25457	34.38925	4,278	340	3,938
CC02232POD1	−103.26411	34.40258	4,317	370	3,947
CC02573POD1	−103.35511	34.43111	4,384	410	3,974
CC02513	−103.32840	34.44839	4,397	387	4,010
CC02356POD1	−103.35581	34.37483	4,296	289	4,007
CC02056POD6	−103.34579	34.41228	4,330	382	3,948
CC01339	−103.30935	34.40201	4,321	360	3,961
CC00865	−103.27973	34.40830	4,328	370	3,958
CC01755	−103.25017	34.38925	4,280	340	3,940
CC02160POD2	−103.29553	34.40372	4,306	330	3,976
CC01477POD3	−103.25025	34.36204	4,239	322	3,917

Hydrogeologic Unit Interpretation

In order to determine the top of Dockum Group (Chinle Formation) (fig. 3), the tops and bases of geologic units (and their hydrogeologic-unit equivalents), hereinafter referred to as "borehole picks," were first determined by analyzing previously published and newly collected lithologic descriptions and borehole geophysical logs. A total of 149 borehole picks were obtained from AECOM (2020), along with 72 borehole picks from NMWRRS (2021) and 43 borehole picks from newly collected TDEM soundings. The data were gridded using Oasis Montaj v. 9.8.1 (Seequent, 2020a) where a kriging method using an exponential variogram model trended to the southeast. Kriging is a geostatistical method that determines the most probable value at each grid node in a 50- by 50-m grid (about 164 ft between nodes in the x and y directions) for this study based on a statistical analysis of the entire dataset (Isaaks and Srivastava, 1989). Variance maps developed during the kriging process were used to evaluate the uncertainty

in hydrogeologic unit surface grids in the planning of additional data-collection tasks. Generally, as the distance between data points became greater, the correlation between the data points decreased, and uncertainty in areas between the data points increased (Isaaks and Srivastava, 1989). Additional information on kriging is available in Isaaks and Srivastava (1989). The contour lines shown in figure 3 were created by using the quick contour method in Oasis Montaj v. 9.8.1 (Seequent, 2020a), are based on available data, and were not adjusted manually. Figure 3 depicts the updated general northwest-to-southeast orientation of the top surface of the Dockum Group (Chinle Formation) that underlies Cannon AFB. The blue-shaded areas in figure 3 correspond to the general location of the paleochannel network, and the result obtained is consistent with the results from previous studies (AECOM, 2020).

Previous base-of-aquifer maps generated for the area have shown areas with water levels below the proposed base of the aquifer; therefore, the area should have been dry. This modified grid compares much better to water level data in the area and has no areas that do not correlate with the other datasets. The minimum saturated thickness in a well that has water level data is approximately 10 ft.

A map of the grid error (variance) derived from the kriging method was developed to depict where possible data gaps may still exist (fig. 4). The updated map of the top of Dockum Group has many areas of uncertainty greater than 20 ft (fig. 4) because there are not enough data for the gridding process to reliably determine a value. However, this interpretation of the altitude of the top of the Dockum Group represents a substantial improvement in data resolution compared to previous studies. The resolution over the entire study area improved because of the additional borehole data, and the resolution along the large paleochannel trending northwest-to-southeast across Cannon AFB is greatly improved by the addition of new, tightly spaced TDEM soundings. Many data gaps are still indicated (fig. 4), and additional data collection is needed to further improve the accuracy with which the top of the Dockum Group is depicted in areas where data remain sparse. Areas within Cannon AFB that would benefit most from additional data collection are in locations where infrastructure hindered the collection of additional TDEM soundings. The depiction of the top of the Dockum Group in areas east and south of the Cannon AFB may benefit from additional TDEM soundings, including areas where difficulty accessing private land hindered data collection.

Paleochannel Analysis

Two methodologies were used to evaluate paleochannels in the top of the Dockum Group across the study area: (1) trend-removal grid analysis and (2) analysis with Esri's ArcMap Hydrology toolset. Trend-removal grids were developed by removing the third-order regional trend from all the data points within the top of Dockum Group (Chinle Formation) surface grids (Seequent, 2020b). Essentially, this technique removes the regional dip of the layer prior to the process of creating surface grids. The resulting trend-removal grid (fig. 5) shows changes in the top of the Dockum Group after the regional trend was removed. Relatively low altitude values represent low-altitude data points in the top of Dockum Group (Chinle Formation) surface grid, and continuous stretches of these low-altitude values can be indicative of paleochannels. Figure 5 shows the same general northwest-to-southeast trend of paleochannel network across Cannon AFB, but with the regional trend removed, it highlights relatively deeper portions of the paleochannels. The areas in figure 5 with darker blues indicate the portions of paleochannels that are substantially deeper (more than 20 ft) relative to the main paleochannel. These deeper areas of the paleochannel indicate portions with greater saturated thickness.

The second paleochannel analysis, performed using Esri's ArcMap Hydrology toolset, treated the surface grid representing the top of the Dockum Group as a digital surface elevation model and simulated a topographic watershed across the surface to identify the location and spatial characteristics of the paleochannel network. The toolset was used to determine the flow direction, flow accumulation, and stream order (Esri, 2021). Ultimately, the toolset simulates the movement of water across a land surface, which for this study corresponds to the top of the Dockum Group surface grid (fig. 3).

Concentric "bullseye" shapes were present in the top of Dockum Group surface contours that were not smoothed manually. For the toolset to function properly, these "bullseyes" (which act as sinks) had to be filled to render the raster hydrologically correct. Next, a flow-direction grid was created to find directional flow between cells and then used as input to the flow-accumulation tool, where a threshold lower than the default value was chosen to identify paleochannel flow paths (Esri, 2021). This flow-accumulation grid was then converted to vector format, where artifacts of the process were removed manually. The final product is a map depicting flow paths (fig. 5) based on the interpolated and smoothed top of Dockum Group altitudes. Data from previous USGS studies were used to check the results from the two methodologies used to evaluate paleochannels in the top of the Dockum Group across the study area.

These two paleochannel analysis techniques show groundwater flow direction as well as areas with the deepest saturated thickness. Hydrologically, these techniques show where aquifer storage is highest (in the deepest parts of the paleochannel network), as well as the spatial distribution of preferential groundwater flow paths (the paleochannels [fig. 5]). The analyses indicate a large paleochannel trending to the southeast with smaller channels feeding in from the west. Areas where groundwater management could be more beneficial are indicated by locations where these flow lines intersect the deeper parts of the paleochannel.

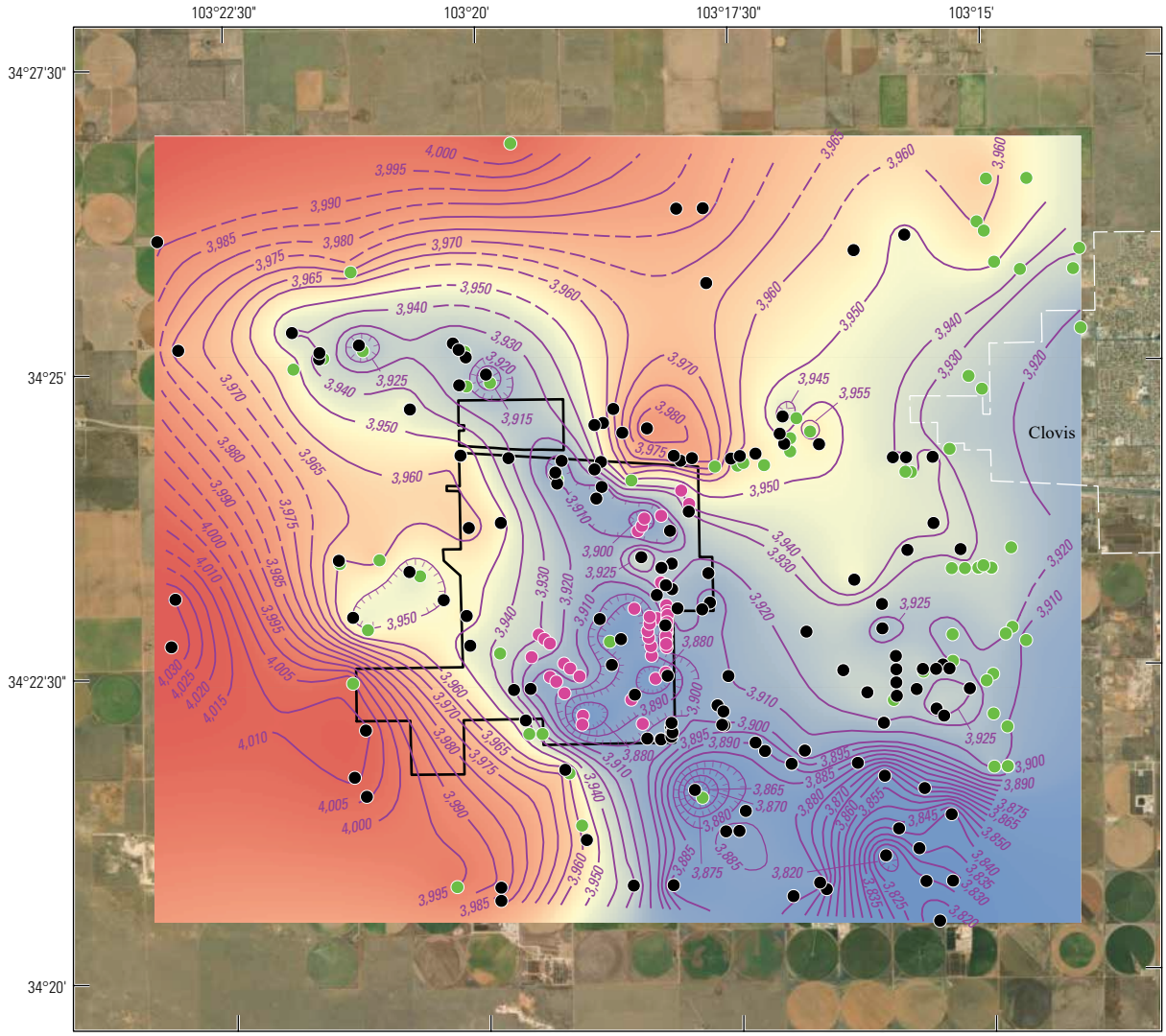

Figure 3. Locations of all boreholes and time-domain electromagnetic (TDEM) soundings with interpreted top of Dockum Group grid and bedrock contours depicting the top surface of the Dockum Group (Chinle Formation) on and near Cannon Air Force Base, Curry County, New Mexico, 2020.

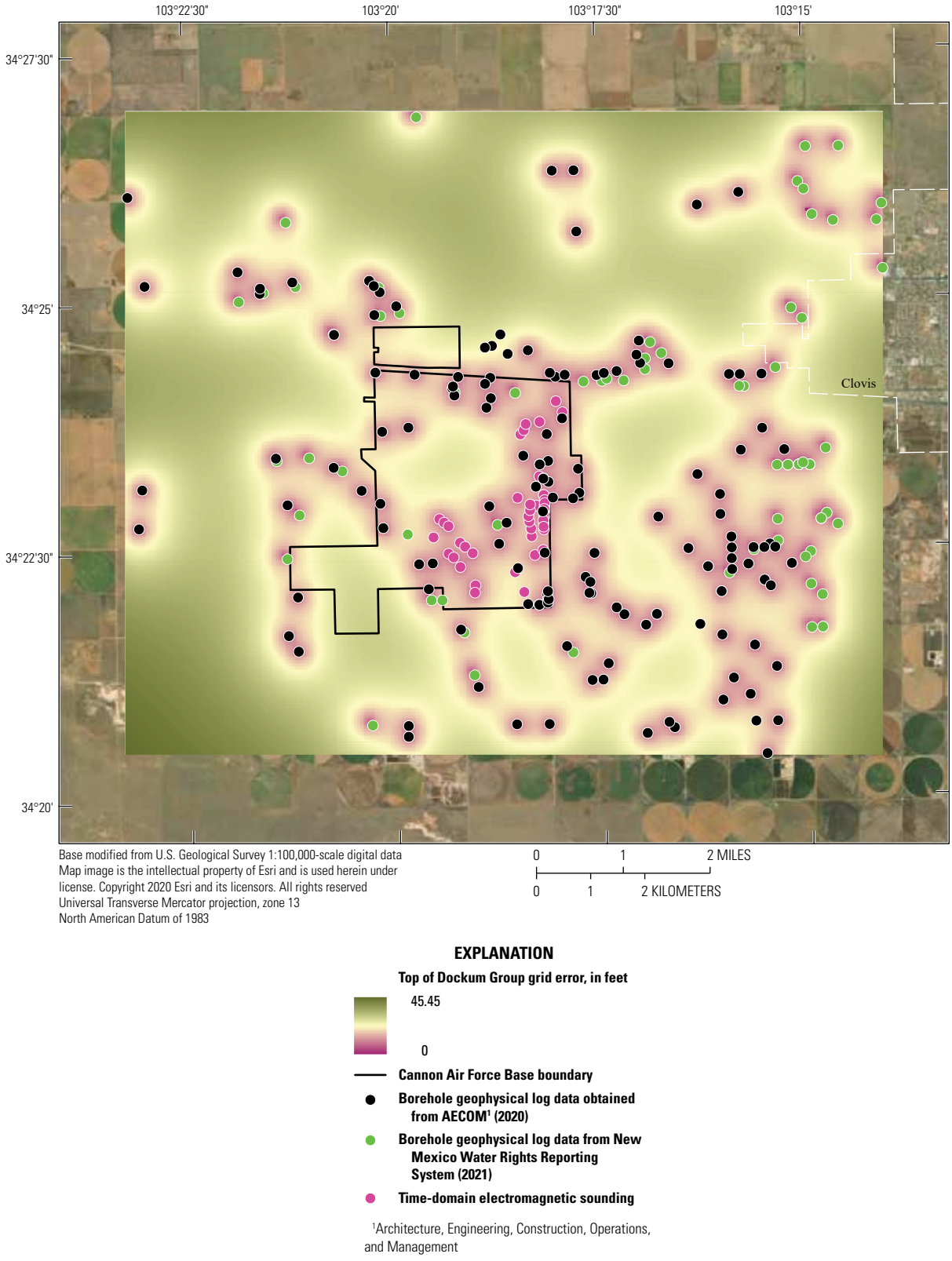

Figure 4. Gridding error of top of Dockum Group (map shown in fig. 3) on and near Cannon Air Force Base in Curry County, New Mexico, 2020.

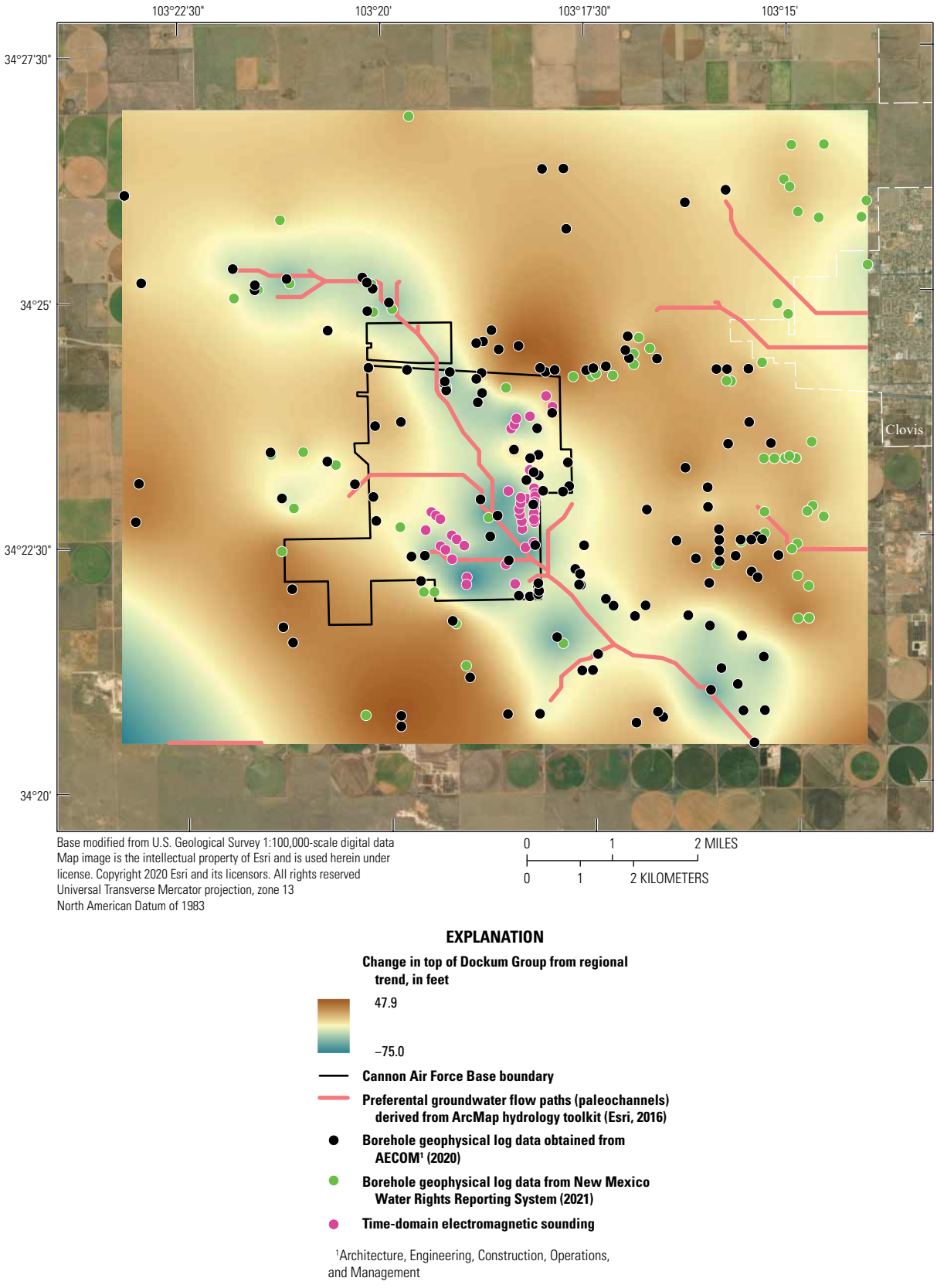

Figure 5. Change in the top of Dockum Group after regional trend was removed and flow lines derived from ArcMap Hydrology toolkit on and near Cannon Air Force Base in Curry County, New Mexico, 2020.

Summary

The hydrogeology on and near Cannon Air Force Base (AFB) was assessed to gain a better understanding of preferential groundwater flow paths through paleochannels. The Southern High Plains aquifer is contained in the Tertiary-age Ogallala Formation in the part of eastern New Mexico where Cannon AFB is located. The Triassic-age Chinle Formation of the Dockum Group underlies the unconfined Southern High Plains aquifer. The Southern High Plains aquifer is the primary source of water for agriculture and public supply in the area, with the sandstone and shale aquifer serving as a minor source of water mostly for agricultural uses. In and near the study area, paleochannels incised the top surface of the Dockum Group (Chinle Formation) and subsequently filled in with electrically resistive coarse-grained sediments of the overlying Ogallala Formation, resulting in a preferential groundwater flow path in the form of a paleochannel network. A better understanding of the spatial characteristics of this preferential groundwater flow path is needed to support ongoing efforts to remediate groundwater contamination at Cannon AFB. Therefore, the U.S. Geological Survey, in cooperation with the U.S. Air Force Civil Engineer Center, used surface geophysical resistivity methods and data compiled from previous studies to better understand the spatial distribution and characteristics of the paleochannel network incised into the top of the Dockum Group.

Previous studies have shown with increasing resolution how paleochannels incised the top of the Dockum Group, but limited borehole data on and near Cannon AFB continued to make accurately mapping the top of Dockum Group challenging. For this study, surface geophysical resistivity measurements in the form of time-domain electromagnetic (TDEM) soundings made by the U.S. Geological Survey were used in conjunction with data previously published by Architecture, Engineering, Construction, Operations, and Management and borehole data compiled from the New Mexico Water Rights Reporting System database to prepare an updated map of the top of the Dockum Group that includes the location and characteristics of paleochannels incised into the top of the Dockum Group (Chinle Formation). A total of 149 borehole picks were obtained from previous studies, along with 72 additional borehole picks from the New Mexico Water Rights Reporting System database and 43 borehole picks from newly collected TDEM soundings. The data were gridded and contoured using Oasis Montaj v. 9.8.1 where a kriging method using an exponential variogram model trended to the southeast was used. A map of the grid error (variance) derived from the kriging method was developed to depict where possible data gaps may still exist. The updated map of the top of Dockum Group has many areas of uncertainty greater than 20 feet because there are not enough data for the gridding process to reliably determine a value. However, this interpretation of the altitude of the top of the Dockum Group represents a substantial improvement in data resolution compared to previous studies. The resolution over the entire study area improved with the additional borehole data, and the resolution along the large paleochannel trending northwest-to-southeast across Cannon AFB is greatly improved by the addition of new, tightly spaced TDEM soundings. Many data gaps remain, and additional data collection is needed to further improve the accuracy with which the top of the Dockum Group is depicted in areas where data remain sparse.

Two methodologies were used to evaluate paleochannels in the top of the Dockum Group across the study area: (1) trend-removal grid analysis and (2) analysis with Esri's ArcMap Hydrology toolset. Trend-removal grids were developed by removing the third-order regional trend from all the point values within the top of Dockum Group (Chinle Formation) surface grids. The resulting trend-removal grid shows changes in the top of the Dockum Group after the regional trend was removed. Relatively low values represent low-altitude points in the top of Dockum Group (Chinle Formation) surface grid and continuous stretches of these low-altitude points can be indicative of paleochannels. The grid shows the same general northwest-to-southeast trend of paleochannel network across Cannon AFB, but with the regional trend removed, it highlights relatively deeper portions of the paleochannels (more than 20 feet relative to the main paleochannel). These deeper areas of the paleochannel indicate areas with more saturated thickness. Esri's ArcMap Hydrology toolset was used to determine the flow direction, flow accumulation, and stream order of paleochannels. A flow-direction grid was first created to find directional flow between cells, then used as input to the flow-accumulation tool, where a threshold lower than the default value was chosen to identify paleochannel flow paths. The final product is a map depicting flow paths based on the interpolated and smoothed top of Dockum Group altitudes. These two paleochannel analysis techniques show groundwater flow direction as well as areas with the deepest saturated thickness. Hydrologically, these techniques show where aquifer storage is highest (in the deepest parts of the paleochannel network), as well as the spatial distribution of preferential groundwater flow paths (the paleochannels). The analyses indicate a large paleochannel trending to the southeast with smaller channels feeding in from the west. Areas where groundwater management could be more beneficial are indicated by locations where these flow lines intersect the deeper parts of the paleochannel.

References Cited

Architecture, Engineering, Construction, Operations, and Management [AECOM], 2020, Cannon Air Force Base conceptual site model Curry County, New Mexico: AECOM technical memorandum AR 2784, 35 p., accessed May 3, 2022, at https://ar.afcec-cloud.af.mil/.

American Society of Testing and Materials, 1999, Standard guide for selecting surface geophysical methods: American Society of Testing and Materials (ASTM) D 6429–99, 11 p.

Becker, M.F., Bruce, B.W., Pope, L.M., and Andrews, W.J., 2002, Ground-water quality in the central High Plains aquifer, Colorado, Kansas, New Mexico, Oklahoma, and Texas, 1999: U.S. Geological Survey Water-Resources Investigations Report 02–4112, 64 p., accessed May 10, 2021, at https://doi.org/10.3133/wri20024112.

Cannon Air Force Base, 2022, 27th Special Operations Group of the United States Airforce: Cannon Air Force Base web page, accessed March 8, 2022, at https://www.cannon.af.mil/Units/27th-Special-Operations-Group/.

Chandra, S., Choudhury, J., Maurya, P.K., Ahmed, S., Auken, E., and Verma, S., 2020, Geological significance of delineating paleochannels with AEM: Exploration Geophysics, v. 51, no. 1, p. 74–83, accessed November 10, 2021, at https://doi.org/10.1080/08123985.2019.1646098.

Collison, J., 2016, Potentiometric surfaces, summer 2013 and winter 2015, and select hydrographs for the Southern High Plains aquifer, Cannon Air Force Base, Curry County, New Mexico: U.S. Geological Survey Scientific Investigations Map 3352, 2-p. pamphlet, accessed December 9, 2021, at https://doi.org/10.3133/sim3352.

Constable, S.C., Parker, R.L., and Constable, C.G., 1987, Occam's inversion—A practical algorithm for generating smooth models from electromagnetic sounding data: Geophysics, v. 52, no. 3, p. 289–300. [Also available at https://doi.org/10.1190/1.1442303.].

Cronin, J.G., 1969, Groundwater in the Ogallala Formation in the Southern High Plains of Texas and New Mexico: U.S. Geological Survey Hydrologic Atlas 330, 9 p., accessed December 9, 2021, at https://doi.org/10.3133/ha330.

Dutton, A.R., and Simpkins, W.W., 1986, Hydrogeochemistry and water resources of the Triassic lower Dockum Group in the Texas Panhandle and eastern New Mexico: Austin, Tex., University of Texas, Bureau of Economic Geology Report of Investigations, no. 161, 51 p., accessed May 11, 2022, at https://store.beg.utexas.edu/reports-of-investigations/2698-ri0161.html.

Esri, 2021, ArcGIS Pro help: Esri web page, accessed April 28, 2021, at https://pro.arcgis.com/en/pro-app/latest/help/main/welcome-to-the-arcgis-pro-app-help.htm.

Fenneman, N.M., and Johnson, D.W., 1946, Physiographic divisions of the conterminous U.S.: U.S. Geological Survey Map, scale 1:7,000,000, accessed November 9, 2021, at https://water.usgs.gov/GIS/metadata/usgswrd/XML/physio.xml.

Geonics Limited, 2006, Products–TEM47: Mississauga, Ontario, Canada, Geonics Limited web page, accessed April 12, 2021, at http://www.geonics.com/html/tem47.html.

Gustavson, T.C., and Holliday, V.T., 1985, Depositional architecture of the Quaternary Blackwater Draw and Tertiary Ogallala Formations, Texas Panhandle and eastern New Mexico: Austin, Tex., University of Texas, Bureau of Economic Geology Open-File Report OF–WTWl–1985–23, 60 p.

Gustavson, T.C., 1996, Fluvial and eolian depositional systems, paleosols, and paleoclimate of the upper Cenozoic Ogallala and Blackwater Draw Formations, Southern High Plains, Texas and New Mexico: Austin, Tex., University of Texas, Bureau of Economic Geology Report of Investigations no. 239, 62 p.

Gutentag, E.D., Heimes, F.J., Krothe, N.C., Luckey, R.R., and Weeks, J.B., 1984, Geohydrology of the High Plains aquifer in parts of Colorado, Kansas, Nebraska, New Mexico, Oklahoma, South Dakota, Texas, and Wyoming: U.S. Geological Survey Professional Paper 1400–B, 63 p., accessed February 16, 2022, at https://doi.org/10.3133/pp1400B.

Interpex Limited, 1996, IX1D version 3 1D sounding inversion: Golden, Colo., Interpex Limited software release, accessed on April 27, 2021, at http://www.interpex.com/ix1dv3/ix1dv3.htm.

Isaaks, E.H., and Srivastava, R.M., 1989, An introduction to applied geostatistics: New York, Oxford University Press, 561 p.

Keller, G.V., and Frischknecht, F.C., 1966, Electrical methods in geophysical prospecting: New York, Pergamon Press, 517 p.

Knowles, T., Nordstrom, P., and Klemt, W.B., 1984, Evaluating the groundwater resources of the High Plains of Texas: Texas Department of Water Resources Report 288, v. l, 178 p., accessed November 9, 2021, at https://www.twdb.texas.gov/publications/reports/numbered_reports/doc/R288/R288v1/R288v1.pdf.

Langman, J.B., Gebhardt, F.E., and Falk, S.E., 2004, Groundwater hydrology and water quality of the Southern High Plains aquifer, Melrose Air Force Range, Cannon Air Force Base, Curry and Roosevelt Counties, New Mexico, 2002–03: U.S. Geological Survey Scientific Investigations Report 2004–5158, 42 p., accessed November 9, 2021, at https://doi.org/10.3133/sir20045158.

Langman, J.B., Falk, S.E., Gebhardt, F.E., and Blanchard, P.J., 2006, Groundwater hydrology and water quality of the Southern High Plains aquifer: U.S. Geological Survey Scientific Investigations Report 2006–5280, 61 p., accessed November 9, 2021, at https://doi.org/10.3133/sir20065280.

Lucas, S.G., Hunt, A.P., and Hayden, S.N., 1987, The Triassic system in the Dry Cimarron Valley, New Mexico, Colorado and Oklahoma, *in* Lucas, S.G., and Hunt, A.P., eds., Northeastern New Mexico: New Mexico Geological Society, Guidebook 38, p. 97–777, accessed May 11, 2022, at https://nmgs.nmt.edu/publications/guidebooks/downloads/38/38_p0097_p0117.pdf.

Lucius, J.E., Langer, W.H., and Ellefsen, K.J., 2007, An introduction to using surface geophysics to characterize sand and gravel deposits: U.S. Geological Survey Circular 1310, 33 p. [Also available at https://doi.org/10.3133/cir1310.]

Luckey, R.R., and Becker, M.F., 1999, Hydrogeology, water use, and simulation of flow in the High Plains aquifer in northwestern Oklahoma, southeastern Colorado, southwestern Kansas, northeastern New Mexico, and northwestern Texas: U.S. Geological Survey Water-Resources Investigations Report 99–4104, 66 p., accessed July 1, 2021, at https://doi.org/10.3133/wri994104.

Mandache, C., and Brothers, M., 2005, Time domain lift-off compensation method for eddy current testing: e-Journal of NDT, v. 10, no. 6, 1 p., accessed June 13, 2022, at https://www.ndt.net/article/v10n06/mandache/mandache.htm.

Matherne, A.M., and Stewart, A.M., 2012, Characterization of the hydrologic resources of San Miguel County, New Mexico, and identification of hydrologic data gaps, 2011: U.S. Geological Survey Scientific Investigations Report 2012–5238, 44 p., accessed November 9, 2021, at https://doi.org/10.3133/sir20125238.

McGowen, J.H., Granata, G.E., and Seni, S.J., 1977, Depositional systems, uranium occurrence and postulated groundwater history of the Triassic Dockum Group, Texas Panhandle-eastern New Mexico: U.S. Geological Survey, 157 p., prepared by the Austin, University of Texas, Bureau of Economic Geology, Austin Tex. under grant no. 14-08-001-G410, accessed May 9, 2022, at https://www.beg.utexas.edu/files/publications/contract-reports/CR1977-McGowen-1.pdf.

McLemore, V.T., 2001, Oasis State Park, *in* Lucas, S.G., and Ulmer-Scholle, D.S., eds., Geology of Llano Estacado: Socorro, N. Mex., New Mexico Geological Society, p. 34–37.

Neuendorf, K.K.E., Mehl, J.P., Jr., and Jackson, J.A., eds., 2005, Glossary of geology (5th ed.): Alexandria, Va., American Geological Institute, 779 p.

New Mexico Interstate Stream Commission and New Mexico Office of the State Engineer, 2016, Lower Pecos Valley Regional Water Plan: Interstate Stream Commission, 264 p., accessed March 20, 2017, at http://www.ose.state.nm.us/Planning/RWP/Regions/10_Lower%20Pecos/2016/Reg%2010_Lower%20Pecos%20Valley_Regional%20 Water%20Plan%20December%202016.pdf.

New Mexico Water Rights Reporting System [NMWRRS], 2021, New Mexico Water Rights Reporting System: New Mexico Office of the State Engineer online database, accessed January 15, 2021, at http://nmwrrs.ose.state.nm.us/nmwrrs/wellSurfaceDiversion.html.

Payne, J.D., and Teeple, A.P., 2020, Surface geophysical data used for mapping the top of the Dockum Group on Cannon Air Force Base in Curry County, New Mexico, 2020: U.S. Geological Survey data release, https://doi.org/10.5066/P9P6KWR5.

Rawlings, G.C., 2016, A hydrogeologic investigation of Curry and Roosevelt Counties, New Mexico: New Mexico Bureau of Geology and Mineral Resources Open-file Report 580, 47 p.

Robson, S.G., and Banta, E.R., 1995, Ground water atlas of the United States—Segment 2, Arizona, Colorado, New Mexico, Utah: U.S. Geological Survey Hydrologic Investigations Atlas 730–C, 34 p., accessed January 23, 2020, at https://doi.org/10.3133/ha730C.

Seequent, 2020a, Oasis Montaj (ver. 9.8.1, August 2020): Seequent software release, accessed April 27, 2021, at https://www.seequent.com/products-solutions/geosoft-oasis-montaj/.

Seequent, 2020b, Regional trend removal: Broomfield, Calif., Seequent, web page accessed October 27, 2020, at https://www.seequent.com/products-solutions/geosoft-oasis-montaj/gridknit-extension.

Tuan, Y.F., Everard, C.E., and Widdison, J.G., 1969, The climate of New Mexico: Santa Fe, N. Mex., New Mexico State Planning Office, 169 p.

U.S. Climate Data, 2021, 1981–2010 Clovis New Mexico weather averages: U.S. climate data web page, accessed August 9, 2021, at https://www.usclimatedata.com/climate/clovis/new-mexico/united-states/usnm0070.

U.S. Geological Survey, 2017, 1 meter digital elevation models (DEMs)—USGS National Map 3DEP downloadable data collection: U.S. Geological Survey data release, accessed December 5, 2021, at https://www.sciencebase.gov/catalog/item/543e6b86e4b0fd76af69cf4c.

U.S. Government Accountability Office, 2021, Report to Congressional Committees—Firefighting foam chemicals: U.S. Government Accountability Office web page, accessed March 8, 2022, at https://www.gao.gov/assets/gao-21-421.pdf.

Vignesh, A., Ramanujam, N., Kumar, B.S., and Rasool, Q.A., 2015, Application of time domain electromagnetic (Tdem) methods for mapping of salt freshwater intrusions and evaluate the porosity in Carbyn's Cove, Wandoor and Khurumedhera Beaches in South Andaman: Journal of Coastal Zone Management, v. 18, no. 4, 5 p., accessed November 9, 2021, at https://doi.org/10.4172/2473-3350.1000413.

For more information about this publication, contact
Director, Oklahoma-Texas Water Science Center
U.S. Geological Survey
1505 Ferguson Lane
Austin, TX 78754-4501
For additional information, visit
https://www.usgs.gov/centers/ot-water
Publishing support provided by
Lafayette Publishing Service Center

ISSN 2328-0328 (online)
https://doi.org/10.3133/sir20225050